Reac Kinet Mech Cat (2016) 117:521–536
DOI 10.1007/s11144-016-0974-0

Effect of aging on the CO oxidation properties of copper manganese oxides prepared by hydrolysis–coprecipitation using tetramethyl ammonium hydroxide

Hisahiro Einaga[1] · **Akihiro Kiya**[1]

Received: 7 September 2015 / Accepted: 4 January 2016 / Published online: 21 January 2016

Abstract Copper manganese mixed oxides were prepared by a hydrolysis-coprecipitation method using tetramethyl ammonium hydroxide and calcined at 573–873 K. The effect of aging treatment after the coprecipitation process on the catalytic properties of the calcined mixed oxides for CO oxidation was investigated. XRD and EXAFS studies showed that spinel phases were mainly formed in the aged catalysts and the degree of disorder in the Cu–Mn spinel oxide phases increased. The aging treatment suppressed the formation of crystallites of mixed oxides, but the treatment promoted the crystallization of impurity CuO phase. The aged catalyst exhibited higher activity for CO oxidation than the unaged catalysts. The optimum calcination temperature for obtaining the highest activity was changed by aging treatment. Refluxing during the aging treatment led to the detrimental effect on the CO oxidation activities.

Keywords Copper–manganese oxides · Hydrolysis–coprecipitation · CO oxidation · Effect of aging

Introduction

Catalytic CO oxidation has become one of the important techniques in industrial and environmental processes. The optimum catalyst composition for catalytic CO oxidation is different depending on the reaction conditions such as reaction temperatures and substrate concentration. At relatively low temperatures, noble

Electronic supplementary material The online version of this article (doi:10.1007/s11144-016-0974-0) contains supplementary material, which is available to authorized users.

✉ Hisahiro Einaga
einaga.hisahiro.399@m.kyushu-u.ac.jp

[1] Department of Energy and Material Sciences, Faculty of Engineering Sciences, Kyushu University, Kasuga, Fukuoka 816-8580, Japan

metal catalysts have been frequently used [1], but they are expensive and generally suffered from deactivation at high temperatures due to metal sintering. On the other hand, transition metal oxides need high temperature for obtaining catalytic activity, although they are inexpensive and showed thermal stability at high temperature.

Copper–manganese (Cu–Mn) mixed oxides are widely used as the oxidation catalysts for various kinds of oxidation reactions [2–5]. They show CO oxidation activity at relatively low temperature [6–11] and are good candidates for substitutes of noble metal catalysts. It is well known that hopcalite catalysts composed of amorphous Cu–Mn phase exhibits CO oxidation activity even at room temperature [12, 13].

Cu–Mn mixed oxides are frequently prepared in the liquid phase from metal complexes by techniques such as the coprecipitation [14, 15], sol–gel [16], and redox methods [17]. In the case of coprecipitation methods, generally, an aqueous solution containing metal nitrates is mixed with precipitation reagents such as sodium carbonates and bicarbonates, and the resulting mixed oxide precursor is calcined to obtain the mixed oxide catalysts. The surface area, crystallinity, oxidation states, which strongly affect the catalytic properties, can be controlled by changing the catalyst composition, additive concentration, metal concentration in the mother liquid, precipitation temperature, final pH values, aging time, and calcination temperature [18–21]. Thus, the textural and catalytic properties of Cu–Mn mixed oxides depend on the preparation conditions.

We have recently reported the preparation methods for Cu–Mn mixed oxides using tetramethyl ammonium hydroxides (TMAH) as a coprecipitation reagent [22]. The catalyst structures and catalytic performance for CO oxidation were investigated. The advantage of this method over the methods using sodium carbonate and sodium bicarbonate was in that it can prevent the formation of the Na-containing impurities in the mixed oxides, which give rise to detrimental effects on the catalytic activities. After calcination at 673 K, the Cu–Mn mixed oxides prepared by our method exhibited higher CO oxidation activity than Cu and Mn single oxides, and the highest activity was obtained at the Cu/Mn ratio of 1/1. EXAFS studies revealed that Cu–Mn spinel oxide phases were mainly formed in the reaction and both Cu and Mn occupied the tetrahedral and octahedral sites.

It has also been reported that in the precipitation methods, the aging of the catalyst precursors in the preparation medium strongly affects the structures and catalytic properties of Cu–Mn mixed oxides [19]. The results in these precedent papers urged us to investigate the effect of aging of the catalyst precursors in the preparation medium. In this paper, we describe the aging of the precipitates was also effective in the hydrolysis-precipitation methods for preparation of Cu–Mn oxides using TMAH. The optimized conditions for the preparation procedure were identified.

Experimental

Catalyst preparation

Cu-Mn mixed oxides with the Cu/Mn ratio of 1/1 were prepared by a precipitation method. 0.020 mol of $Cu(NO_3)_2{\cdot}3H_2O$ (Wako Pure Chemical, Japan, >99.9 %) and

0.020 mol of $Mn(NO_3)_2{\cdot}6H_2O$ (Wako Pure Chemical, Japan, >99.9 %) were dissolved into pure water (100 mL). The solution was added dropwise to 100 mL of 10 %-tetramethylammonium hydroxide solution (Kishida Chemical Co., Ltd.) under vigorous stirring. The resulting metal hydroxide particles were left in the solution for 20–72 h. The colloidal particles were filtered off, washed with water, dried at 373 K for 24 h, and calcination at 573–873 K for 5 h.

Catalyst characterization

X-ray diffraction (XRD) patterns were obtained using a RIGAKU RINT2200 diffractometer using Cu K_α radiation at 40 kV and 30 mA. N_2 adsorption isotherms were measured at 77 K using Belsorp mini series (BEL Japan Co. Ltd.) Surface areas of the samples were determined by the Brunauer–Emmett–Teller (BET) method from the N_2 adsorption isotherm. The morphologies of the samples were analyzed by scanning electron microscopy (JEOL JSM-6340F).

XAFS spectra were obtained at Kyushu University beamline in the Kyushu Synchrotron Light Research Center (SAGA-LS/BL-06). The spectra were obtained at room temperature. The data reduction of experimental absorption spectra was carried out according to the method recommended by the Standards and Criteria Committee of the International XAFS Society [23] using a REX2000 software (ver.2.60). Detailed procedures for data reduction were reported in the previous paper [22]. k^3-weighted EXAFS data ($k^3\chi(k)$) were Fourier transformed to R-space over 3.0–15.8 $Å^{-1}$ for Mn K-edge and 2.3–14.0 $Å^{-1}$ for Cu K-edge spectra. EXAFS curve fitting was performed using theoretical backscattering amplitude and phase shift functions calculated by the program FEFF8 [24].

XPS spectra were recorded with a Kratos ESCA-3400 spectrometer with a Mg K_α source (1253.6 eV). The binding energies were corrected using the values of 284.8 eV for the C 1 s peak of the carbon species on the catalyst samples as an internal standard.

Catalytic CO oxidation

The catalytic oxidation of CO was carried out with a fixed bed flow reaction system. For a pretreatment, 0.050 g of Cu–Mn mixed oxide catalyst in a U-shaped glass reactor was heated at 573 K in an O_2 flow for 1 h. The reaction was carried out at 343 K with a gas composition (CO 0.5 %–O_2 0.25 %–He balance). Gas samples were analyzed on a GC-TCD (Shimadzu GC-14B). The rate for CO oxidation was determined under the condition that the CO conversion was linear to the catalyst weight divided by gas flow rate.

Results and discussion

Structural changes in Cu–Mn oxides after aging

In our previous paper, we demonstrated that Cu–Mn oxides were prepared by a hydrolysis-coprecipitation method using TMAH as a pH regulator. After the

aqueous solution containing metal nitrates was added dropwise to the TMAH-containing solution, the resultant precipitates were filtered off, dried, and calcined at 673 K to obtain the Cu–Mn oxides. EXAFS studies revealed that Cu–Mn mixed oxides having spinel phases were formed in this preparation process. The spinel type mixed oxides exhibited higher activity for CO oxidation in the temperature range of 343–403 K.

In the present study, we investigated the effect of aging treatment on the properties of Cu–Mn mixed oxides. After the precipitates were prepared by the hydrolysis-coprecipitation method using TMAH, they were aged in the precipitation medium for 20–72 h at room temperature prior to the post-treatment. Fig. 1 shows the effect of aging time on the surface area of Cu–Mn oxide after calcination. The surface areas of the unaged oxide were approximately 90 and 60 $m^2\ g^{-1}$ after calcination at 573 and 673 K, respectively. The catalyst surface areas increased after 20 h aging, and further increase in aging time slightly improved the surface area. Thus, the surface areas of the calcined oxides were improved by the aging treatment.

Fig. 2 shows the FE-SEM images of the aged and unaged Cu–Mn oxides calcined at 673 K. The Cu–M mixed oxides were composed of aggregates of spherical particles with the sizes smaller than 200 nm and highly sintered larger particles. The images also show that the morphologies of the oxides were not so much influenced by the aging treatment.

The aging of oxide precursors also affected the crystal structures of the calcined Cu–Mn oxides. Fig. 3 shows the XRD patterns of Cu–Mn mixed oxides prepared by the hydrolysis–coprecipitation method using TMAH, followed by calcination at

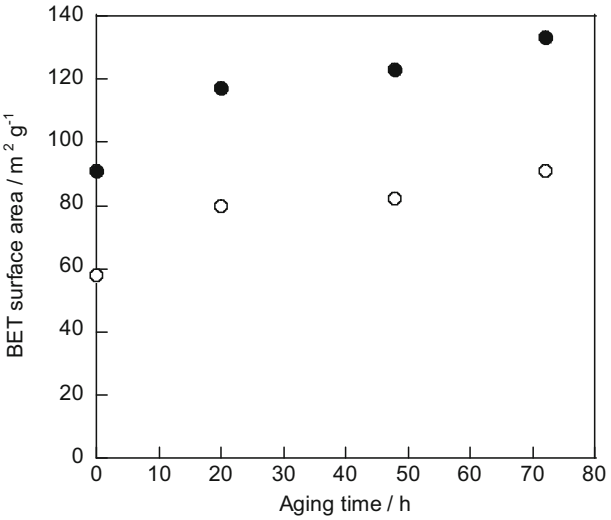

Fig. 1 Effect of aging time on surface area of Cu–Mn mixed oxides prepared by hydrolysis-coprecipitation with TMAH, followed by calcination at 573 (*filled circle*) and 673 K (*empty circle*) for 5 h in air

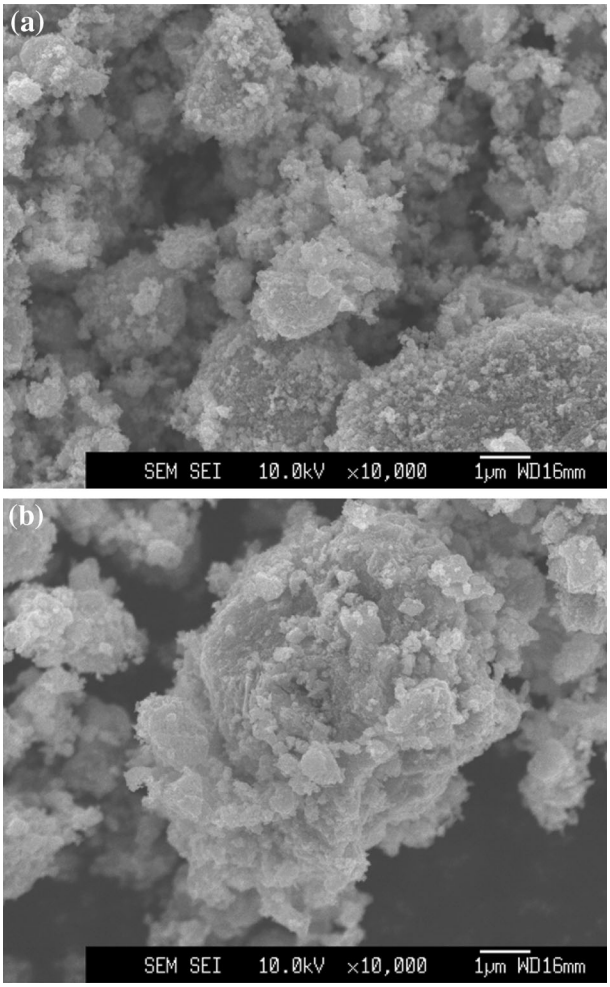

Fig. 2 FE-SEM images of Cu–Mn mixed oxides prepared by hydrolysis–coprecipitation with TMAH, followed by 673 K for 5 h. **a** Without aging, and **b** with aging for 20 h

673 K for 5 h. For the Cu–Mn mixed oxides obtained without aging treatment, the peaks for $Cu_3Mn_3O_8$ spinel phases were observed, along with the peaks for impurity CuO phases. For the Cu–Mn oxides obtained after the 20 h aging of the precipitates, the peaks for the $Cu_3Mn_3O_8$ spinel phases were also observed, but the peaks were broadened and lower in their intensities than those for the unaged oxides. After 20 h aging, the peak intensities decreased with the increase in aging time and the crystallite size estimated from the Scherrer equation changed from 13.3 to 9.4 nm. When the aging treatment was 72 h, the peaks for Cu–Mn spinel phases slightly increased in their intensities and the crystallite size increased again to 12.5 nm. On the other hand, the peaks for the impurity CuO phases increased as the aging time increased, showing the growth of CuO crystallites in the aging treatment.

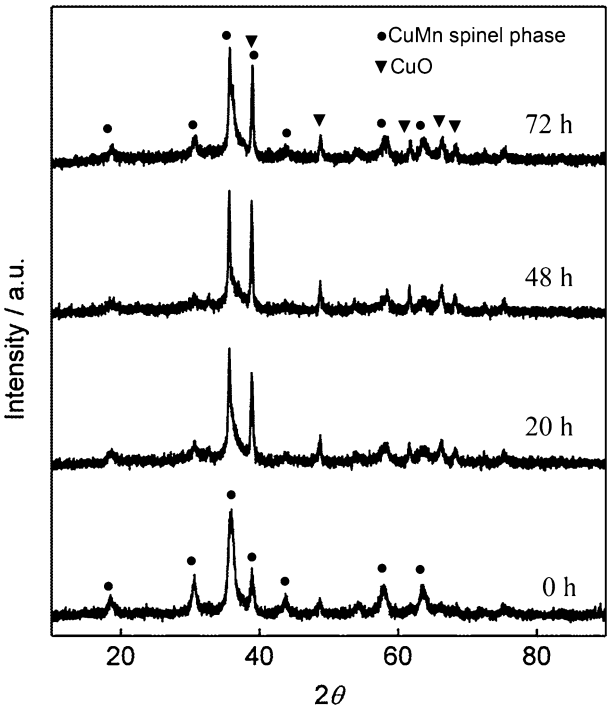

Fig. 3 XRD patterns of Cu–Mn mixed oxides prepared by hydrolysis-coprecipitation with TMAH, followed by calcination at 673 K for 5 h

Although the XRD studies showed that the aging treatment led to the decrease in crystallites of Cu–Mn–O mixed phases, EXAFS studies confirmed that Cu–Mn spinel type mixed phases were mainly formed in the aged oxides. Fig. 4 shows the Mn K-edge EXAFS spectra of the Cu–Mn mixed oxides that were prepared with and without aging treatment (Fig. 4a). For the unaged Cu–Mn oxides, the peaks were observed at 1.56 (phase uncorrected: pu), 2.52 and 3.10 Å (pu). Curve fitting results for the Mn K-edge spectra for the aged oxides are summarized in Table 1. On the basis of the fitting results, the peak at 1.56 Å (pu) was due to the Mn–O bond, whereas the peak at 2.52 Å (pu) was mainly ascribed to the contributions of Mn–Cu and Mn–Mn bonds in Cu–Mn spinel phase [22]. The peak positions were much different from those of Mn single oxides, MnO, Mn_3O_4, Mn_2O_3 and MnO_2 [(SI Fig. S1)]. Therefore, the peaks at 1.56 (pu), 2.52 and 3.10 Å (pu) confirmed the formation of mixed oxide phases. As the aging time increased, the peak intensities for Mn–O, Mn–Cu and Mn–Mn bonds were not significantly changed and the peak positions were almost unchanged. As shown in Table 1, the coordination numbers of these bonds for the aged oxides were close to those for the unaged oxides, indicating that that the spinel phases were also dominant structures in the aged oxides. On the other hand, the Debye–Waller factor, which reflects the thermal and structural disorder of crystallites slightly increased. The observation was consistent

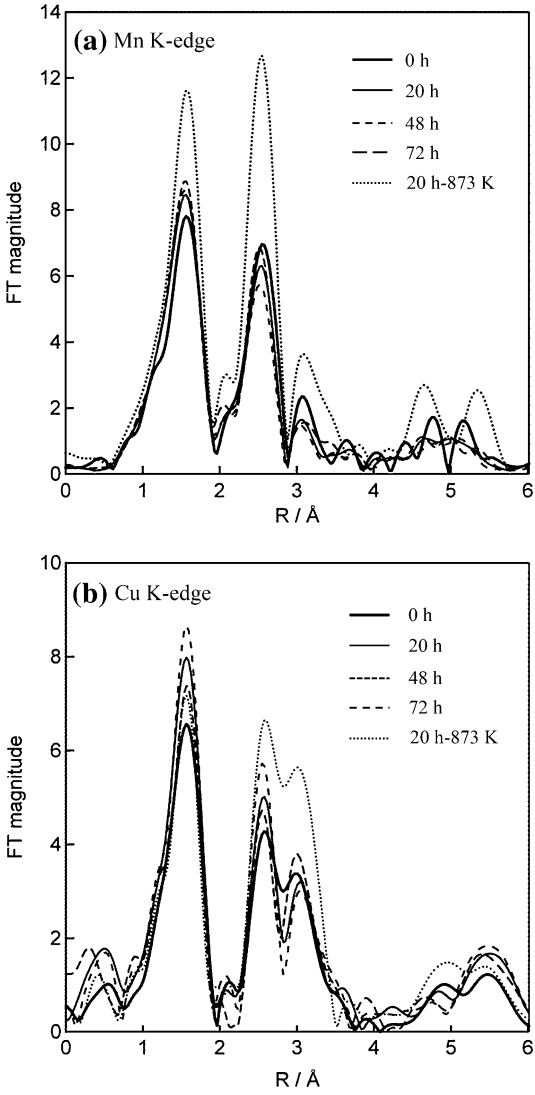

Fig. 4 Effect of aging time on the changes in EXAFS spectra of Cu–Mn mixed oxides prepared by hydrolysis–coprecipitation with TMAH, followed by calcination at 673 K for 5 h. **a** Mn K-edge; **b** Cu K-edge

with that obtained from the XRD studies that crystalline sizes of Cu–Mn spinel type mixed oxides decreased.

Fig. 4 also shows the Cu K-edge EXAFS spectra of Cu-Mn oxides (Fig. 4b). For the unaged Cu–Mn oxides, the peak of Cu–O was observed at 1.56 Å (pu), whereas the peaks at 2.64 and 3.07 Å (pu) were mainly attributable to Cu–Mn and Cu–Cu contributions in Cu–Mn spinel phases. However, CuO phase was also present in the Cu–Mn oxides, and, therefore, curve fitting for Cu K-edge spectra could not be applied to the spectra because the contribution of Cu–Cu bond in the CuO phase to the peaks at 1.56 and 2.64 Å (pu) cannot be neglected. With the increase in aging

Table 1 Mn K-edge EXAFS curve-fitting results for Cu–Mn mixed oxide catalysts

Catalyst	Shell	CN	R/Å	σ^2 10^{-5} nm^2	ΔE/eV	R_f/%[a]
Cu–Mn(1-1)	Mn–O	4.6 ± 0.2[b]	1.929 ± 0.01[b]	6.40[b]	−1.63[b]	1.8[b]
Without aging	Mn–Cu	1.1 ± 0.2[b]	2.900 ± 0.03[b]	5.63[b]	−2.45[b]	
	Mn–Mn	2.3 ± 0.5[b]	2.936 ± 0.03[b]	6.72[b]	−2.12[b]	
20 h	Mn–O	5.0 ± 0.2	1.927 ± 0.01	6.24	−0.35	2.003
	Mn–Cu	1.2 ± 0.2	2.898 ± 0.03	6.89	−0.37	
	Mn–Mn	2.3 ± 0.5	2.936 ± 0.03	7.92	−0.54	
48 h	Mn–O	5.0 ± 0.2	1.920 ± 0.01	6.40	−0.45	3.62
	Mn–Cu	1.0 ± 0.2	2.899 ± 0.03	6.89	−0.49	
	Mn–Mn	2.1 ± 0.5	2.936 ± 0.03	7.40	−0.54	
72 h	Mn–O	4.6 ± 0.2	1.929 ± 0.01	6.40	−1.63	1.77
	Mn–Cu	1.1 ± 0.2	2.900 ± 0.03	5.63	−2.45	
	Mn–Mn	2.3 ± 0.5	2.936 ± 0.03	6.72	−2.12	
20–600 h	Mn–O	5.3 ± 0.2	1.927 ± 0.01	4.36	−2.5530	1.639
	Mn–Cu	1.7 ± 0.2	2.900 ± 0.03	4.62	−2.50	
	Mn–Mn	3.3 ± 0.5	2.936 ± 0.03	5.04	−3.022	

[a] The residual factor: $R_f(\%) = \frac{\sum \left\{k^3\chi(k)_{obs} - k^3\chi(k)_{calc}\right\}^2}{\sum \left\{k^3\chi(k)_{obs}\right\}^2} \times 100$

[b] The data are obtained from Ref. [22]

time, the peak positions were almost unchanged but the intensities for the peaks at 1.56 and 2.64 Å (pu) increased. The changes in the EXAFS spectra imply that the degree of disorder in the local environment around Cu atoms decreased and were consistent with the XRD result that highly-crystallized CuO phase was formed in the aging treatment.

When the aged Cu-Mn oxide was calcined at 873 K, the peak intensities for 1.56 (pu), 2.52 and 3.10 Å (pu) increased in the Mn K-edge spectrum (Fig. 4a). The curve fitting results also confirmed the formation of Cu-Mn spinel phases. The Debye–Waller factor greatly decreased, indicating that the highly-ordered spinel type structures were formed for the oxide calcined at 873 K. This finding was consistent with the observation for the Cu K-edge spectrum that the peaks at 2.64 and 3.07 Å (pu) increased in their intensities.

It has been reported that good linear relationship is observed between the average oxidation state of Mn and the absorption edge in the Mn K-edge XANES spectra [(SI Fig. S2)] [25, 26]. From the relationship, the Mn oxidation state was determined and listed in Table 1. The oxidation state was 3.2 for the aged and unaged catalysts, showing that the oxidation state was also unchanged during the aging process. The value was consistent with the value estimated from the composition of spinel phase $Cu_3Mn_3O_8$. In a separate experiment, we conducted temperature programmed reduction with H_2 for the aged Cu–Mn mixed catalysts. The amount of H_2 consumption was consistent with the values obtained for the composition of $Cu_3Mn_3O_8$, confirming that the catalyst was mainly composed of Cu–Mn spinel phase.

Effect of aging on the surface state of Cu–Mn oxides

X-ray photoelectron spectroscopic studies provided us the information on the surface states of Cu–Mn mixed oxides. Fig. 5 shows the XPS spectra of Cu–Mn mixed oxides prepared by the hydrolysis-coprecipitation method using TMAH and calcined at 673 K. In the range of 635–660 eV, the peaks of Mn were observed with the spin–orbit splitting of Mn $2p_{1/2}$ and Mn $2p_{3/2}$ signals. The Mn $2p_{3/2}$ peak was located in the range of 641.5 ± 0.1 eV, and the peak position was unchanged when the aging time increased. FWHM (full width at half maximum) for the Mn $2p_{3/2}$ signal was close for the aged and unaged oxides.

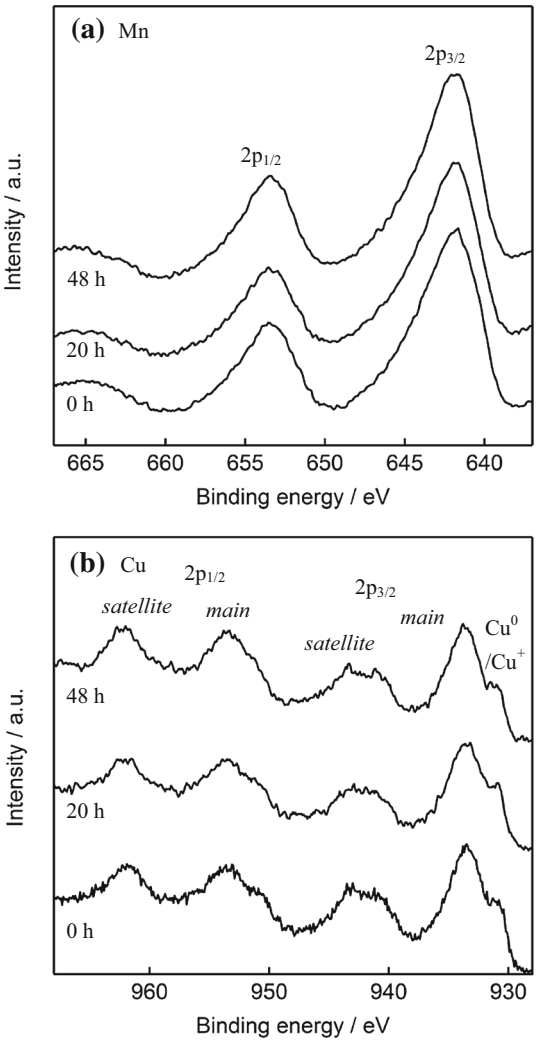

Fig. 5 Changes in the XPS spectra of Cu–Mn mixed oxides prepared by hydrolysis-coprecipitation with TMAH, followed by aging and calcination at 673 K for 5 h. **a** Mn, **b** Cu

For the oxides prepared with aging process, Cu $2p_{1/2}$ and Cu $2p_{3/2}$ peaks for Cu^{2+} species were observed in the range of 930–970 eV (Tables 2, 3), along with satellite peaks due to charge transfer, indicating that Cu^{2+} species were mainly present in the Cu–Mn mixed oxides [27, 28]. The peak due to Cu^{+} (or Cu^{0}) species was also detected at 931.0 eV for the aged and unaged Cu–Mn mixed oxides. Thus, the reduced Cu species (Cu^{0} and Cu^{+}) remained after the aging treatment.

The molar ratios of Mn/Cu for the surface site of the Cu–Mn oxides were estimated from the XPS peak intensities and listed in Table 2. With the increase in aging time, the Mn/Cu ratio increased from 1.6 to 2.3, indicating that the Mn concentration increased by the aging treatment.

Effect of aging on CO oxidation activity

Fig. 6 shows the effect of aging time on the catalytic activity for CO oxidation over Cu–Mn oxides calcined at 673 K. Here, the reaction was carried out at 343 K and the reaction rate per catalyst weight was determined at steady state. The reactions were carried out at low conversion levels (<10 %) where the CO conversions were linear to W/F values. Under such conditions, the effect of mass transfer and heat transfer on the reaction rates was neglected during the reaction. The CO oxidation rate increased with increasing aging time due to the increase in surface area, as shown in Fig. 1. The aging treatment for 24–48 h also improved the CO oxidation rate normalized by surface area. The Cu-Mn oxides obtained after 20 h aging exhibited the CO oxidation rate of 8.1×10^{-6} mol min^{-1} m^{-2} per surface area, which was 1.37 times larger than that with the unaged catalyst. The increase in the CO oxidation activity normalized by surface area can be ascribed to the formation of less-crystallized phases in the Cu–Mn oxides, since the crystallization of the Cu–Mn oxides gives rise to the decrease in oxidizing ability. It should be noted that CuO catalyst prepared by the coprecipitation method did not show the CO oxidation activity at 343 K under our condition.

Fig. 6 also shows that the CO oxidation rate normalized by catalyst weight and that by catalyst surface area decreased with further increase in aging time (72 h), although they were higher than those for unaged catalyst. This behavior can also be explained in terms of the crystallinity of mixed oxide phase. As described above, the crystallite sizes estimated by the Scherrer equation decreased by aging for 20 h, whereas the size increased by further aging (72 h). A similar behavior was observed

Table 2 XPS analysis for Mn 2p peaks Cu–Mn mixed oxides

Aging time h^{-1}	$Mn2p_{3/2}$	$Mn2p_{1/2}$	FWHM for $Mn2p_{3/2}$	Mn/Cu mole ratio	Average oxidation state of Mn
0[a]	641.5[a]	653.4[a]	4.2[a]	1.6[a]	3.2[a]
20	641.5	653.4	4.3	2.2	3.2
48	641.6	653.3	4.3	2.3	3.2

[a] The data are obtained from Ref. [22]

Table 3 XPS analysis for Cu 2p peaks Cu–Mn mixed oxides

Aging time h^{-1}	$Cu2p_{3/2}$	$Cu2p_{3/2}$ satellite	$Cu2p_{1/2}$	$Cu2p_{3/2}$ satellite
0[a]	933.9	943.2	953.2	962.0
20	933.7	943.0	953.6	962.2
48	933.8	943.2	953.5	962.4

[a] The data are obtained from Ref. [22]

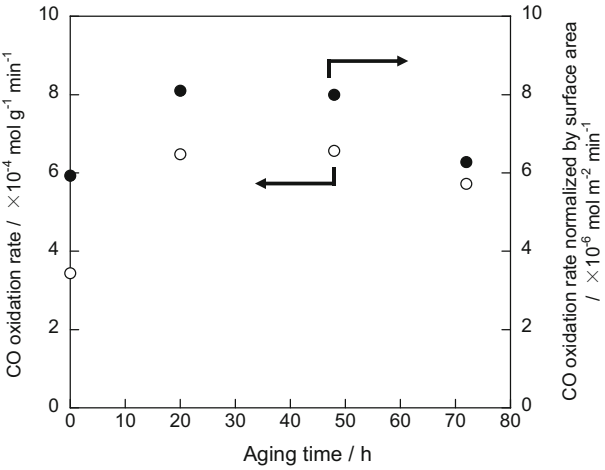

Fig. 6 Effect of aging time on the CO oxidation rate for Cu–Mn mixed oxides calcined at 673 K. Reaction temperature: 343 K. Reaction gas: 0.5 % CO–0.25 % O_2–N_2 balance. Catalyst weight: 0.050 g, gas flow rate: 100–500 mL min^{-1} (WHSV = 120–600 L g^{-1} h^{-1})

for XAFS studies: the Debye–Wallar factor (σ) for Mn–Cu and Mn–Mn bondings (Table 1), which is related to the degree of the order of the crystallites, increased after 20–48 h aging and then decrease after 72 h. These findings suggested that the CO oxidation activities increased with the decrease in the crystalline order of the Cu–Mn spinel phases.

It has been reported that CuO nanopowders have the activity for CO oxidation at temperatures higher than 310–320 K [29]. Therefore, we cannot exclude the possibility that nanosized CuO particles were formed in the Cu–Mn mixed oxides and the tight contact of CuO–$Cu_3Mn_3O_8$ can play in catalytic CO oxidation because CuO crystallites were formed and their sizes increased with increasing the aging time. However, we suggest that Cu–Mn spinel phases contributed to CO oxidation according to the following reasons. First, the Cu–Mn mixed oxides with the Cu/Mn ratio of 1/2 did not contain CuO phase but they showed the activity for CO oxidation in the temperature range of 343–403 K [22]. In addition, XPS studies revealed that the ratio of Cu to Mn on the catalyst surface decreased with decreasing aging time. If we assume that the CuO phase was the only active phase, we cannot explain the results that the catalyst aging enhanced the CO oxidation activity of

Cu–Mn mixed oxides because the amount of CuO species on the surface sites decreased by the treatment.

Effect of heat treatment on the aged catalyst

As described above, the crystal structure of Cu–Mn mixed oxides was affected by the aging treatment. Subsequently, we investigated the effect of calcination temperature on the crystal structure of aged Cu–Mn mixed oxides. Fig. 7 shows the XRD patterns of the Cu–Mn oxides that had been aged for 20 h. The Cu–Mn oxides were calcined in the temperature range of 573–873 K. For the oxides calcined at 573 K, only the peaks for CuO phases were clearly seen in the XRD patterns. As the calcination temperature increased to 673 K, the peaks for $Cu_3Mn_3O_8$ phases appeared and the peak intensities increased with the increase in the calcination temperature. The mixed oxide calcined at 873 K showed distinct peaks for spinel phases were observed, which was consistent with the EXAFS results that highly-ordered spinel phase were formed after 873 K calcination. The peaks for CuO phases diminished after the catalyst was calcined at 873 K, indicating that the impurity CuO phase was reacted as the calcination temperature increased.

Fig. 8 shows the effect of aging treatment on the surface area of the Cu–Mn mixed oxides calcined at various temperatures (Fig. 8a). As the calcination temperature rose, the catalyst surface area decreased monotonically for both the aged and unaged catalysts. The aged catalysts have higher surface area than the unaged catalysts at any calcination temperature, further indicating that the aging treatment was effective in improving the surface area of the Cu–Mn mixed oxides.

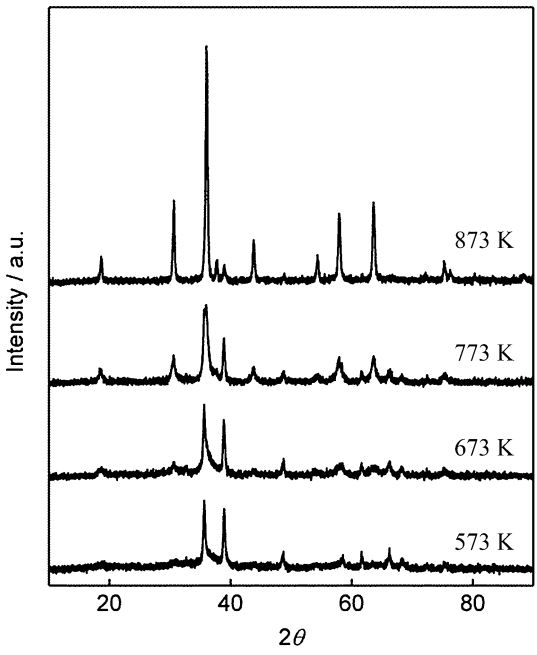

Fig. 7 Effect of calcination temperature on the XRD patterns of 20 h-aged catalysts. Calcination time: 5 h

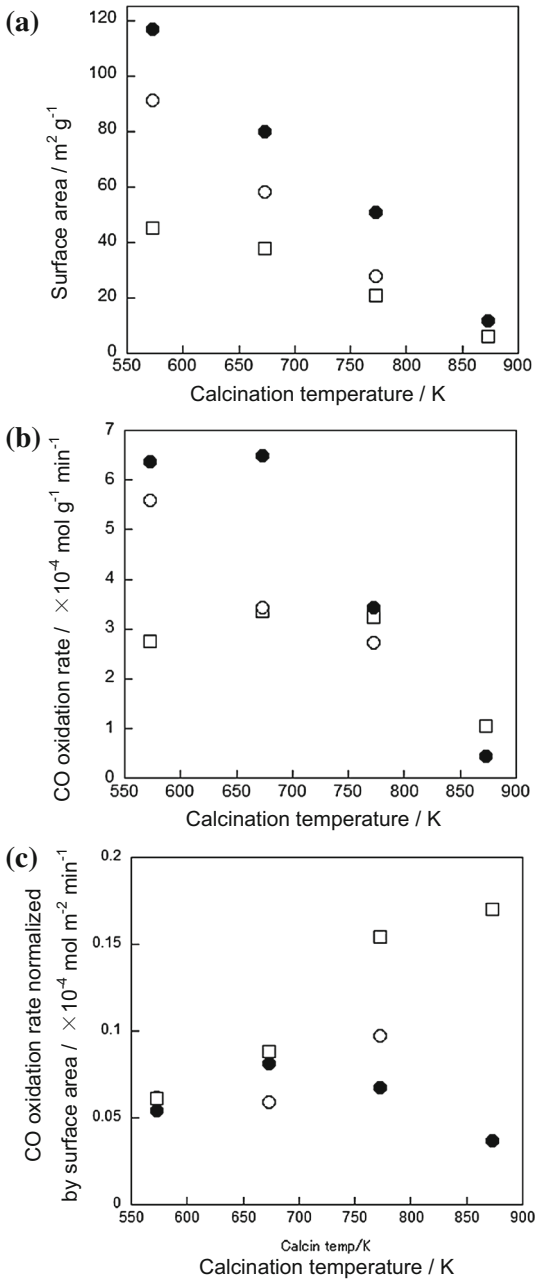

Fig. 8 Effect of calcination temperature on the surface area (**a**), CO oxidation rate (**b**) and CO oxidation rate normalized by surface area (**c**). *Empty circle* unaged catalysts, *filled circle* aged catalysts, and *empty square* refluxed catalysts. Calcination time: 5 h. Reaction temperature: 343 K. Reaction gas: 0.5 % CO–0.25 % O_2–N_2 balance. Catalyst weight: 0.050 g, gas flow rate: 100–500 mL min^{-1} (WHSV = 120–600 L g^{-1} h^{-1})

Fig. 8 also shows the effect of calcination temperature on the CO oxidation rate with Cu–Mn mixed oxides (Fig. 8b). The CO oxidation rate with the unaged catalyst monotonously decreased with the increase in calcination temperature, which was consistent with the behavior of catalyst surface area. On the other hand, for the aged

catalysts, the dependency of catalytic activity on the calcination temperature was inconsistent with that of surface area: the CO oxidation rate slightly increased when the calcination temperature increased to 673 K. As the calcination temperature further increased to 773–873 K, the rate decreased and dropped to the level of the unaged catalysts. Thus, the optimized temperature for catalyst calcination was shifted to higher temperature by the aging treatment. The improved activity of Cu–Mn oxides for CO oxidation by aging treatment was not only ascribed to the enhanced surface area, but also due to the increased CO oxidation rate normalized by surface area, which was related to the structure of Cu–Mn spinel oxide phases. As the aging time increased, the degree of disorder in the Cu–Mn spinel oxide phases, which contributed to CO oxidation, increased, as discussed above. On the other hand, the impurity CuO phases were highly crystallized by the aging treatment, but they did not contribute to the CO oxidation at 343 K [22].

Fig. 9 shows the catalytic activities of Cu–Mn mixed oxides for CO oxidation at various reaction temperatures. The catalysts that had been aged for 20 h and

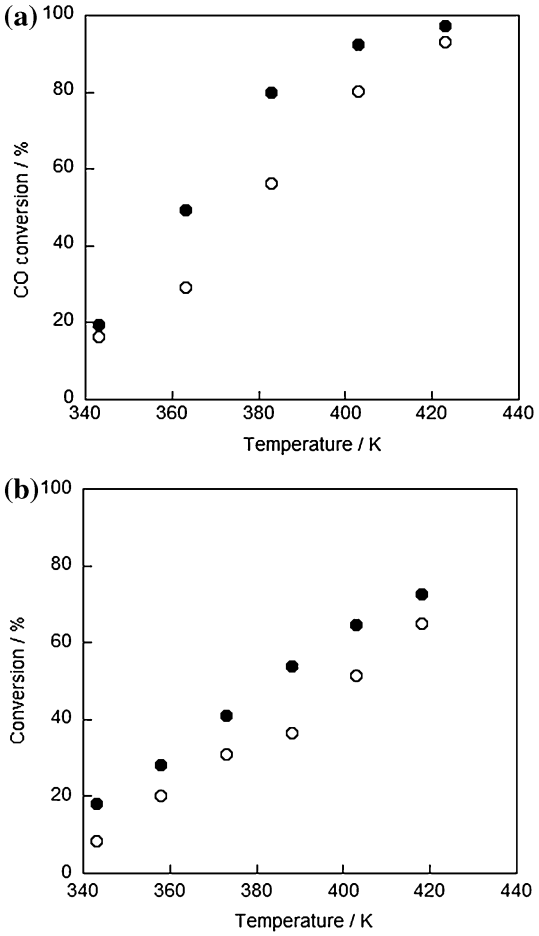

Fig. 9 Effect of temperature on the CO oxidation activity over Cu–Mn mixed oxides. **a** 20 h-aged catalyst, **b** unaged catalyst. Catalyst calcination temperature 673 K. Reaction gas: 0.5 % CO–N_2 balance. Catalyst weight: 0.050 g, gas flow rate: 100 mL min^{-1} (WHSV = 120 L g^{-1} h^{-1}). *Empty circle* 0.25 % O_2; *filled circle* 5.0 % O_2

calcined at 673 K exhibited higher activity than the unaged catalysts at any given temperature.

Effect of heat treatment during aging

As described above, the aging treatment at room temperature improved the catalytic properties of Cu–Mn mixed oxides prepared by hydrolysis-coprecipitation method using TMAH. It has been reported that heating of precipitation medium during the aging treatment affected the surface area of metal oxides prepared by precipitation method [30]. With the increase in the medium temperature during aging treatment, the surface area increased and refluxing of the medium solution was particularly effective for improving the catalyst surface area [30]. These results urged us to investigate the effect of refluxing during the aging process on the Cu–Mn mixed oxides prepared by hydrolysis-coprecipitation method using TMAH. When the Cu–Mn precursor precipitates were refluxed in the precipitation medium for 3 h, the surface areas of the catalysts calcined in the temperature range of 573–873 K were lower than those of the catalysts aged at room temperature (Fig. 8). The CO oxidation activities of the catalysts that had been refluxed and calcined at 573 K were lower than those of the unaged catalysts. As the calcination temperature increased to 673 and 773 K, the CO oxidation activity increased and was comparable with that of aged catalyst. Particularly, the CO oxidation activity normalized by catalyst surface area increased at 773–873 K and was much higher than that for the unaged catalysts. Thus, the optimized temperature was different depending on the aging treatment.

Conclusion

In this study, Cu–Mn mixed oxides were prepared by hydrolysis-coprecipitation method using tetramethylammonium hydroxide. Our results show that the post-treatment process, the aging treatment of mixed oxide precursors in the precipitation medium changed the textural and catalytic properties of the mixed oxides calcined at 673 K. The crystalline sizes of Cu–Mn spinel type mixed oxides which contributed to CO oxidation decreased by aging treatment, whereas the crystalline sizes of CuO, impurity phases increased. The catalytic activity of Cu–Mn mixed oxide for CO oxidation was enhanced by the aging treatment of the oxide precursors. The highest activity was obtained when the aged catalyst was calcined at 673 K. The reflux of the precipitation medium during the aging treatment led to the decrease in the surface area and CO oxidation activity of Cu–Mn mixed oxide calcined at 673 K.

Acknowledgments This study was financially supported by New Energy and Industrial Technology Development Organization.

References

1. Zafiris GS, Gorte RJ (1993) J Catal 140:418
2. Chen H, Tong X, Li Y (2009) Appl Catal A 370:59

3. Li WB, Chu WB, Zhuang M, Hua J (2004) Catal Today 93–95:205
4. Morales MR, Barbero BP, Cadús LE (2008) Fuel 87:1177
5. Njagi EC, Genuino HC, King'ondu CK, Dharmarathna S, Suib SL (2012) Appl Catal A 421–422:154
6. Kondrat SA, Davies TE, Zu Z, Boldrin P, Bartley JK, Carley AF, Taylor SH, Rosseinsky MJ, Hutchings GJ (2011) J Catal 281:279
7. Mirzaei AA, Shaterian HR, Joyner RW, Stockenhuber M, Taylor SH, Hutchings GJ (2003) Catal Commun 4:17
8. Clarke TJ, Davies TE, Kondart SA, Taylor SH (2015) Appl Catal B 165:222
9. Njagi EC, Genuino HC, King'ondu CK, Chen C-H, Horvath D, Suib SL (2011) Int J Hydrog Energy 36:6768
10. Cai L-N, Guo Y, Lu A-H, Branton P, Li WC (2012) J Mol Catal A 360:35
11. Hasegawa Y, Fukumoto K, Ishima T, Yamamoto H, Sano M, Miyake T (2009) Appl Catal B 89:420
12. Rogers TH, Piggot CS, Bahlke WH, Jennings JM (1921) J Am Chem Soc 43:1973
13. Veprek S, Cocke DL, Kehl S, Oswald HR (1986) J Catal 100:250
14. Porta P, Moretti G, Jacono ML, Musicanti M, Nardella A (1991) J Mater Chem 1:129
15. Tang Z-R, Jones CD, Aldridge JKW, Davies TE, Bartley JK, Carley AF, Taylor SH, Allix M, Dickinson C, Rosseinsky MJ, Claridge JB, Xu Z, Crudace MJ, Hutchings GJ (2009) Chem Cat Chem 1:247
16. Hosseini SA, Niaei A, Salari D, Alvarez-Galvan MC, Fierro JLG (2014) Ceram Int 40:6157
17. Njagi EC, Chen C-H, Genuino H, Galindo H, Huang H, Suib SL (2010) Appl Catal B 99:103
18. Hutchings GJ, Mirzaei AA, Joyner RW, Siddiqui MRH, Taylor SH (1996) Catal Lett 42:21
19. Hutchings GJ, Mirzaei AA, Joyner RW, Siddiqui MRH, Taylor SH (1998) Appl Catal A 166:143
20. Jones C, Cole KJ, Taylor SH, Crudace MJ, Hutchings GJ (2009) J Mol Catal A 305:121
21. Porta P, Moretti G, Musicanti M, Nardella A (1993) Solid State Ion 63–65:257
22. Einaga H, Kiya A, Yoshioka S, Teraoka Y (2014) Catal Sci Technol 4:3713
23. Koningsberger DC (1993) Jpn J Appl Phys Suppl 32–2:8
24. Ankudinov AL, Ravel B, Rehr JJ, Conradson SD (1998) Phys Rev B 58:7565
25. Ressler T, Brock SL, Wong J, Suib SL (1993) J Phys Chem B 103:6407
26. Ressler T, Wong J, Roots J, Smith IL (2000) Environ Sci Technol 34:950
27. Pauly N, Tougaard S, Yubero F (2014) Surf Sci 620:17
28. Ghijsen J, Tjeng LH, van Elp J, Eskes H, Westerink J, Sawatzky GA (1988) Phys Rev B 38:11322
29. Svintsitskiy DA, Chupakhin AP, Slavinskaya EM, Stonkus OA, Stadnichenko AI, Koscheev SV, Boronin AI (2013) J Mol Catal A: Chem 368:95
30. Chuah GK, Jaenicke S, Cheong SA, Chan KS (1996) Appl Catal A 145:267–284